

Dispersive micro solid-phase extraction (D $\mu$ SPE) with graphene oxide as adsorbent for sensitive elemental analysis of aqueous samples by laser induced breakdown spectroscopy (LIBS)

F.J. Ruiz, L. Ripoll, M. Hidalgo, A. Canals



PII: S0039-9140(18)30856-7  
DOI: <https://doi.org/10.1016/j.talanta.2018.08.044>  
Reference: TAL18965

To appear in: *Talanta*

Received date: 16 May 2018  
Revised date: 9 August 2018  
Accepted date: 16 August 2018

Cite this article as: F.J. Ruiz, L. Ripoll, M. Hidalgo and A. Canals, Dispersive micro solid-phase extraction (D $\mu$ SPE) with graphene oxide as adsorbent for sensitive elemental analysis of aqueous samples by laser induced breakdown spectroscopy (LIBS), *Talanta*, <https://doi.org/10.1016/j.talanta.2018.08.044>

This is a PDF file of an unedited manuscript that has been accepted for publication. As a service to our customers we are providing this early version of the manuscript. The manuscript will undergo copyediting, typesetting, and review of the resulting galley proof before it is published in its final citable form. Please note that during the production process errors may be discovered which could affect the content, and all legal disclaimers that apply to the journal pertain.

# Dispersive micro solid-phase extraction (D $\mu$ SPE) with graphene oxide as adsorbent for sensitive elemental analysis of aqueous samples by laser induced breakdown spectroscopy (LIBS)

F. J. Ruiz\*, L. Ripoll, M. Hidalgo\* and A. Canals

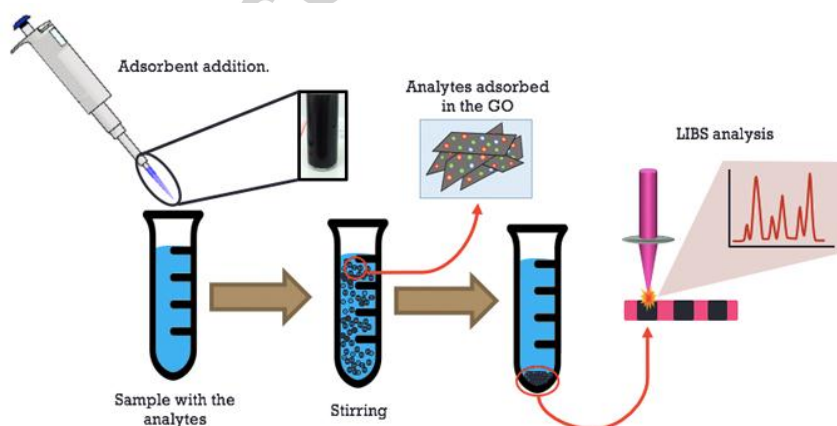
Department of Analytical Chemistry and Food Sciences and University Materials Institute,  
University of Alicante, E-03690, Alicante, Spain

\* Corresponding authors. Tel.: +34 965903400 (Ext. 2421). E-mail addresses:  
montserrat.hidalgo@ua.es (M. Hidalgo); ruiz.espinar@ua.es (F. J. Ruiz).

## Abstract

In this work, the combination of dispersive micro solid-phase extraction (D $\mu$ SPE) with laser-induced breakdown spectroscopy (LIBS) was evaluated for simultaneous preconcentration and detection of Zn, Cd, Mn, Ni, Cr and Pb in aqueous samples. Two adsorbent materials were tested in the microextraction step, namely graphene oxide and activated carbon. In both cases, the microextraction process consisted in the dispersion of a small quantity of adsorbent in the sample solution containing the analytes. However, while the use of activated carbon required a previous chelation of the metals, this step was avoided with the use of graphene oxide. After extraction, the analytes retained in the adsorbents were analysed by LIBS. Several experimental factors affecting the extraction of the metals (adsorbent amount, pH and extraction time) were optimized by means of the traditional univariate approach. Under optimum microextraction conditions, the analytical features of the proposed D $\mu$ SPE-LIBS methods were assessed, leading to limits of detection below 100  $\mu\text{g kg}^{-1}$  and 50  $\mu\text{g kg}^{-1}$  with the use of activated carbon and graphene oxide, respectively, as adsorbents in the D $\mu$ SPE process. Trueness evaluation of the most sensitive procedure was carried out by spike and recovery experiments in a real sample of tap water, leading to recovery values in the range 98% -110%.

## Graphical abstract:



**Keywords:** Dispersive micro solid-phase extraction, graphene oxide, LIBS, trace analysis, liquid samples

Electronic supplementary material available.

## 1. Introduction

Information on the elemental composition of liquids is of major concern in many real world applications encompassing vastly different fields. Because of the huge demand for this chemical information, elemental analysis in analytical chemistry is greatly developed nowadays. As a result, current analytical procedures based on the use of well-established instrumental techniques are able to perform accurate and sensitive elemental analysis of liquid samples. For instance, routine laboratory analysis of liquids by flame atomic absorption spectroscopy (FAAS), inductively coupled plasma atomic emission spectroscopy (ICP-OES), electrothermal atomic absorption spectroscopy (ETAAS) or inductively couple plasma mass spectroscopy (ICP-MS) can provide quantitative information of major-to-ultratrace elements in a sample. Despite the progress in elemental analysis, emerging challenges of modern society place new demands on analytical chemistry. Particularly, there is a growing need for ever-faster analytical results (*e.g.*, in real-time), with chemical analysis preferably performed *in-situ*. In response to these emerging demands, the trend of today's analytical chemistry is shifting toward the development of portable and fully automated analytical systems, able to replace the sophisticated, expensive and bulky laboratory instruments in those applications needing *in situ* and real time analysis [1]. In the specific case of elemental analysis of liquids, portable systems are of special interest in many situations, such as the continuous monitoring of water bodies pollution, or the uninterrupted quality control of beverages during a manufacturing process, to give some examples. In this context, laser-induced breakdown spectroscopy technique (LIBS) has particular characteristics that fulfil many of the requirements for a portable analytical system. LIBS instrumentation can be of small size and completely automatic. In addition, LIBS measurements are very fast and can be carried out in atmospheric conditions [2]. Despite its advantages for *in situ* and real time applications, the high limits of detection characterizing LIBS technique is a major drawback, particularly when liquid samples are the target. In an attempt to overcome this problem, different strategies for LIBS measurement of liquids have been developed by many authors. For instance, it has been proved that LODs are largely improved when LIBS measurements are performed on the surface of a liquid or on liquid jets, aerosols or isolated droplets, in comparison with those performed in the bulk liquid [3, 4]. In addition, further improvements can be achieved by using the double-pulse LIBS modality (DP-LIBS) [5, 6]. The application of some of the abovementioned strategies has allowed the detection of several alkaline and alkaline earth metals in liquids at the  $\mu\text{g L}^{-1}$  level [5, 7, 8]. However, many other relevant analytes with high health and environmental impact (*e.g.*, Cd, Cr, Pb, etc.) can only be detected at the  $\text{mg L}^{-1}$  or hundreds of  $\mu\text{g L}^{-1}$  level [6, 9-11]. An alternative route to improve limits of detection in LIBS is the

application of sample preparation procedures. Concretely, the use of Solid Phase Extraction (SPE) processes can improve the quantitative capability of LIBS for liquid samples analysis, leading to LODs at the low  $\mu\text{g L}^{-1}$  levels [12, 13]. In recent years, a new modality of SPE, denoted as Solid Phase Microextraction (SPME), is being increasingly used. SPME utilizes a very small amount of solid for extraction (i.e., of the order of  $\mu\text{g}$ ) and therefore minimizes the consumption of adsorbent and can lead to a faster extraction process compared to the traditional SPE. Nowadays, there is a wide diversity of possible SPME configurations, such as Stir Bar Sorptive Extraction (SBSE), Dispersive micro Solid-Phase Extraction (D $\mu$ SPE) or Thin-Film Microextraction (TFME), among others [14-16]. Moreover, there is also a wide variety of materials that can be used as solid adsorbents; from the classical activated carbon or silica-gel to the most modern nanomaterials, such as ordered mesoporous silica, silica nanoparticles, carbon nanotubes, graphene or metal-organic frameworks (MOFs), among others [16, 17]. Despite the great versatility and high potential of SPME procedures, this extraction modality has been scarcely investigated as sample preparation procedure for liquid samples analysis by LIBS. To date, and to the authors' knowledge, Wang *et al.* [18] have been the only researchers combining SPME with LIBS detection. In Wang *et al.* work, extraction of different metals from aqueous solutions was performed by using D $\mu$ SPE modality and graphite nanoparticles as adsorbent material. Before extraction, metals in the samples were previously chelated to improve the species' affinity for the adsorbent, and LIBS analysis of the analyte-enriched solids resulting from this D $\mu$ SPE procedure allowed the detection of Ag, Mn and Cr at concentrations below  $17 \mu\text{g L}^{-1}$ . The results obtained by these authors demonstrated the capability of SPME procedures to improve LIBS LODs in the analysis of liquids, however, more research is still needed in order to fully exploit the potential of the SPME-LIBS hyphenation. Some examples are investigations of new adsorbents able to improve the extraction capacity and/or to simplify the microextraction procedure (*e.g.*, high surface area and/or functionalized adsorbents), or studies of different SPME modalities with great possibilities for future automation.

In this work, graphene oxide (GO) was evaluated as a possible adsorbent able to simplify the SPME process in analytical procedures based on the SPME-LIBS hyphenation. The choice of GO was based on the very high theoretical surface area characterizing these kind of materials ( $2630 \text{ m}^2 \text{ g}^{-1}$  for a monolayer of graphene) and, in special, on the presumable ability of GO for direct extraction of metal ions due to the presence of oxygen-containing functionalities on the solid surface. In order to evaluate the possible advantage of using GO as adsorbent in the SPME procedure, the results obtained with this material were compared to that obtained with the use of activated carbon (AC). AC was selected as reference adsorbent due to its extensive use for the removal of pollutants in water and air remediation processes, its high surface area for adsorption and its low cost. With the use of these two adsorbents, different analytes (*i.e.*, Zn, Cd, Mn, Ni, Cr and Pb) were extracted from aqueous samples by using D $\mu$ SPE modality. D $\mu$ SPE was chosen among the several existing SPME modalities due to its relative experimental simplicity, which allowed for a fast testing and comparison of the adsorbents. After the extraction procedures, the analyte-enriched adsorbents were analysed by LIBS. As a first step, the main experimental factors affecting the D $\mu$ SPE procedures were optimized using univariate optimization. Under optimum D $\mu$ SPE conditions, analytical figures of merit of the D $\mu$ SPE-LIBS procedures developed with the two adsorbents were

estimated. Finally, trueness was evaluated for the most efficient  $\mu$ SPE-LIBS procedure by spiking-recovery assays on a real sample of tap water.

## 2. Experimental

### 2.1. Instruments and apparatus

#### 2.1.1. LIBS measurements

The LIBS experimental setup used in this work is schematically shown in Fig. 1. The laser-induced plasmas were generated in air at atmospheric pressure with a pulsed Nd:YAG laser (Handy-YAG, HYL 101, Q-switched, Quanta System S.P.A., Italy), emitting pulses of energy 150 mJ (6 ns FWHM pulse width) at the fundamental wavelength ( $\lambda=1064$  nm) and 10 Hz repetition rate. The laser was focused onto the sample by a 60 mm focal length plano-convex lens. Plasma emission was collected at  $60^\circ$  with respect to the laser beam axis by a five-furcated optical fibre ( $5 \times 400$   $\mu$ m fibre optic cable, FC5-UV400-2, Avantes, The Netherlands), and was sent to the entrance slit of a five-channel spectrometer (AvaSpec-2048-SPU, Avantes, the Netherlands) equipped with 2048 pixel CCD array detectors, where plasma's light was spectrally resolved and detected. LIBS measurements were externally controlled by manually triggering the laser firing (*i.e.*, external triggers to laser flashlamp and Q-switch) with two pulse generators (Digital delay/pulse generator, DG 535, Stanford Research Systems, Inc.; and 1 MHz–50 MHz pulse/function generator, 8116A, Hewlett Packard/Agilent Technologies, USA). Synchronization of laser firing and data acquisition was performed with the same two-pulse generators system and with the aid of the spectrometer software (AvaSoft<sup>®</sup>, v 8.5.0.0, Avantes, The Netherlands). All LIBS spectra were collected 1.3  $\mu$ s after the plasma generation, with 1 ms acquisition time. Zn II (202.50 nm), Cd II (214.44 nm), Mn II (259.37 nm), Cr I (357.87 nm), Ni I (352.45 nm) and Pb I (368.35 nm) were the emission lines evaluated in this work.

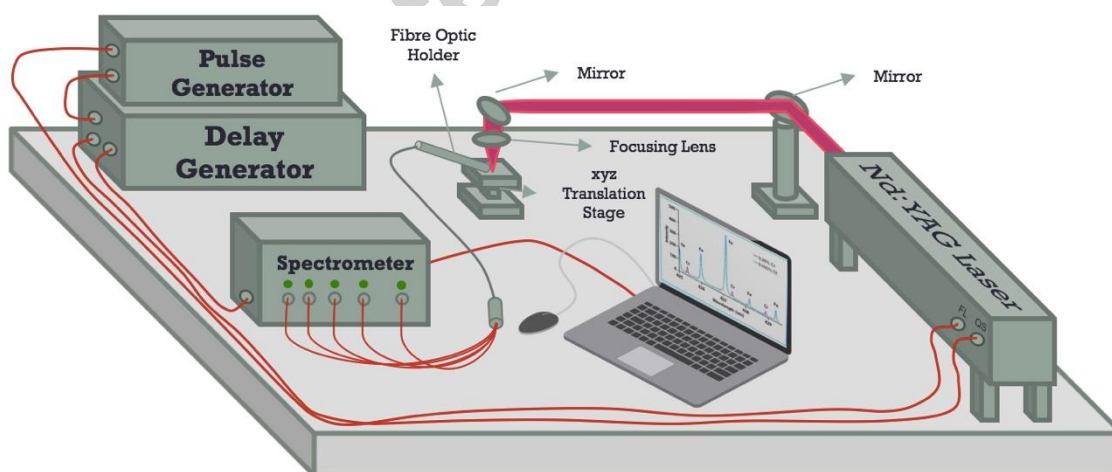


**Fig. 1** Scheme of the LIBS experimental setup.

#### 2.1.2. Microextraction procedures

Adjustment and measurement of the solutions pH was carried out using a pH meter (Basic 20+, Crison Instrument, Spain). Aqueous dispersions of GO were prepared with the use of an ultrasonic bath

(Transsonic TP690, Elma Company, Germany). A hotplate stirrer (501, Darlab Egara S.L., Spain) was used to accelerate the mass transfer in the microextraction processes. The same hotplate was employed to dry the analyte-enriched adsorbents after the extraction processes and prior to LIBS analyses. After extractions, the adsorbents were separated from the samples using a centrifuge (2690/5, Nahita Centrifuges, Spain).

### 2.1.3. Characterization of activated carbon and graphene oxide adsorbents

The morphology of both AC and GO adsorbents was examined using a scanning electron microscope (SEM) (S3000N, Hitachi High-Technologies Corporation, Japan) and a transmission electron microscope (TEM) (JEM-2010, JEOL Ltd., Japan). Surface area and pore size analysis was carried out through adsorption-desorption studies. To this end, adsorption-desorption isotherms of N<sub>2</sub> at 77K and of CO<sub>2</sub> at 273K were obtained with a volumetric adsorption device (Autosorb-6, Quantachrome Instruments, USA). The samples (*i.e.*, 100 mg of the solid adsorbents) were previously degassed for 4 h at 523 K and  $5 \cdot 10^{-5}$  bar by using a degassing unit (Autosorb Degasser, Quantachrome Instruments, USA). Isotherms analysis by the Brunauer-Emmett-Teller (BET) and Dubinin-Radushkevich models was made with the software package of Quantachrome (*i.e.*, Autosorb<sup>®</sup> software provided with the Autosorb-6 device). Identification of functional groups was investigated through Attenuated Total Reflectance Fourier Transform Infrared spectroscopy (ATR-FTIR), with the use of a Fourier transform infrared spectrometer (FTIR 4700, Jasco Analytica Spain S.L., Spain).

## 2.2 Reagents and solutions

All solutions were prepared with analytical grade chemicals and deionized water obtained from a water purification system (Seta Osmo BL-6, Grupo SETA, Spain). Standard aqueous solutions containing Zn (II), Cd (II), Mn (II), Cr (III), Ni (II) and Pb (II) were prepared by appropriate dilution of 1000  $\mu\text{g g}^{-1}$  high-purity mono-element stock solutions (High-Purity standards, UK). Diluted ammonia and nitric acid solutions (0.25% (w/w)), prepared from extra pure 32% (w/w) ammonia solution (Sharlab S.L., Spain) and reagent grade 60% (w/w) nitric acid solution (Sharlab S.L., Spain), respectively, were used for pH adjustment. Sodium diethyldithiocarbamate trihydrate (DDTC) ( $\geq 99.0\%$  purity, Sigma Aldrich, USA) was used as chelating agent in D $\mu$ SPE procedures using activated carbon as adsorbent. A real sample of tap water collected from the drinking water supply system of Alicante (Spain) was used for evaluation of the analytical method trueness.

Activated carbon (canister type) was synthesized and furnished to our group by the Carbon Materials and Environment research group at the University of Alicante (Spain), while graphene oxide was a commercial product purchased from Sigma Aldrich (Graphene oxide flakes, Sigma Aldrich, USA). For the D $\mu$ SPE procedures, the adsorbents (*i.e.*, AC or GO) were added to the samples from previously prepared aqueous dispersions having 5 mg mL<sup>-1</sup> solid concentration. In the case of activated carbon, the solid was previously sieved through a 63  $\mu\text{m}$  laboratory test sieve (Cisa Cedaceris Industrial S.L., Spain) in order to remove coarse particles. The activated carbon aqueous suspension was manually shaken until homogeneous particle dispersion was visually observed (see Fig. 2). After shaking, the dispersion was stable during approximately one hour. In the case of graphene oxide, previous sieving was unnecessary due to its reduced particle size. However, the prepared suspension was sonicated during 15 min in an

ultrasonic bath in order to separate the graphene oxide layers and to obtain a well-distributed dispersion of the solid. Both AC and GO dispersions were visually similar immediately after preparation, but GO dispersion was stable during a much longer time (*i.e.*, about one day).

## 2.3 Experimental procedure

AC and GO were tested in parallel as adsorbent materials for the detection of different analytes from water samples by using the proposed D $\mu$ SPE-LIBS analytical methodology. In both cases, analytes were first extracted from the samples and concentrated in a small quantity of adsorbent (Section 2.3.1), which was subsequently analysed by LIBS (Section 2.3.2). For the sake of clarity, D $\mu$ SPE procedures carried out with the use of AC and GO as adsorbents have been denoted as D $\mu$ SPE(AC) and D $\mu$ SPE(GO), respectively, throughout the text, while the whole measurement procedures (*i.e.*, D $\mu$ SPE followed by LIBS detection) have been denoted as D $\mu$ SPE(AC)-LIBS and D $\mu$ SPE(GO)-LIBS. All the results presented in this work are the mean of three replicate analysis performed through the whole measurement procedures.

### 2.3.1 D $\mu$ SPE procedure

Due to the different physical-chemical characteristics of AC and GO adsorbents, slightly different experimental procedures were applied for metal extraction using D $\mu$ SPE(AC) and D $\mu$ SPE(GO) modalities. Activated carbon is known to be relatively free from oxygen-containing functional groups in surface (see section 3.1 below) and, therefore, a limited capacity for metal ions adsorption was to be expected. For this reason, a chelation step using DDTc as chelating agent was included in the D $\mu$ SPE(AC) procedure, with the aim to enhance the adsorption efficiency for the target analytes when in the form of metal-DDTC complexes. Graphene oxide, by contrast, can be characterized by its ambivalent hydrophobic/hydrophilic nature, allowing the adsorption of both organic compounds and metal ions [19]. Due to the presence of oxygen-containing functionalities on the GO surface, successful removal of metal ions from aqueous solutions has been reported by many authors, without the need of any previous metal complexation step [20-23]. For this reason and looking for the greatest possible simplification of the microextraction procedure, metal chelation was avoided in the D $\mu$ SPE(GO) process.

The general experimental procedure for extraction of the analytes by D $\mu$ SPE is illustrated in Fig. 2. In the D $\mu$ SPE(AC) procedure, approximately 10 g of sample was deposited in a 15 mL test tube and the solution pH was adjusted with diluted ammonia and nitric acid solutions. A given quantity of activated carbon was mixed with the sample by addition of the corresponding volume of a previously prepared 5 mg mL<sup>-1</sup> adsorbent suspension, which was always shaken during 3 min in a vortex mixer immediately prior to use. Subsequently, an excess amount of chelating agent was added to the mixture (*i.e.*, 0.5% (w/w) of DDTc), and then the solution weight was brought to 11 g with deionized water. The so prepared mixture was stirred for a certain time, and finally was centrifuged during 3 min at 3000 rpm. After centrifugation, the resulting analyte-enriched adsorbent was collected from the bottom of the test tube with a micropipette and was conveniently prepared for LIBS analysis.

The D $\mu$ SPE(GO) procedure was essentially similar to that described for D $\mu$ SPE(AC) with the exception of the chelation step, as previously pointed out.

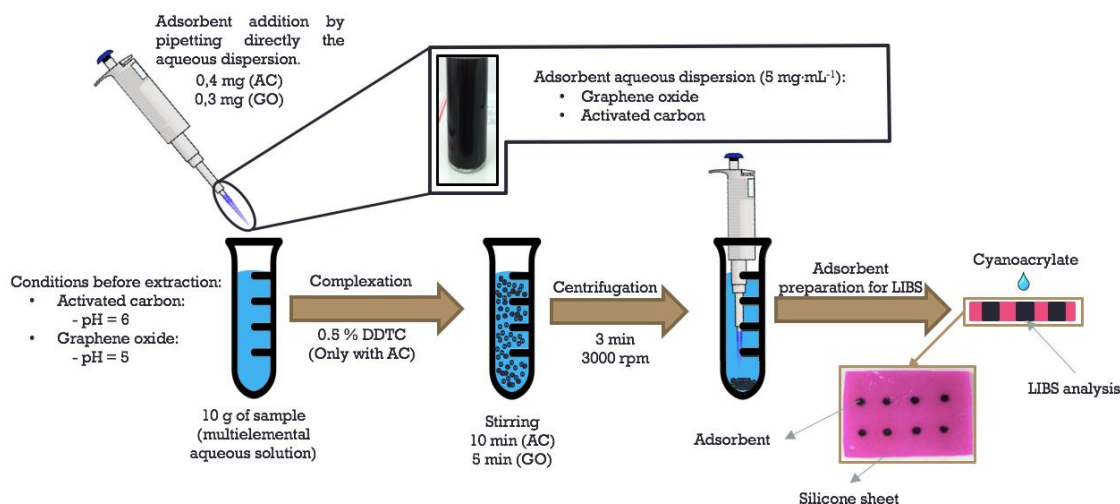


Fig. 2 Scheme of the microextraction procedure.

### 2.3.2 LIBS analysis of the adsorbents

For LIBS analysis, the solid phase resulting from the microextraction procedure was placed in a circular mould fabricated in commercial silicone sheets (see Fig. 2) and, once in the mould, the adsorbent was heated to dryness in a hotplate. Afterward, in order to immobilize the fine powdery solid and to avoid particles spreading under laser irradiation during LIBS measurements, a small drop of cyanoacrylate glue was added to the adsorbent. A preliminary analysis of cyanoacrylate glue by LIBS revealed no spectral interferences with the target analytes, as can be observed from Fig. S1. LIBS measurements were performed by averaging the signal of the maximum number of laser shots needed to ablate completely the solid, in both surface and depth. The number of laser shots per LIBS analysis was mainly dependent on the type of adsorbent studied (*i.e.*, AC or GO) and on the dimension of the silicone mould. Unless otherwise stated, LIBS analysis of AC was performed by averaging 100 laser shots (*i.e.*, 10 different surface locations with 10 shots in each location), and GO analysis was performed by averaging 80 laser shots (*i.e.*, 10 different surface locations with 8 shots in each location).

## 3. Results and discussion

### 3.1 Characterization of the adsorbents

The textural parameters of activated carbon and graphene oxide obtained from the N<sub>2</sub> and CO<sub>2</sub> adsorption-desorption isotherms are listed in Table S1. As shown in the Table, the AC framework contains micropores and mesopores in nearly similar proportion, which can both contribute to the adsorption of the target analytes in the form of metal chelates. The specific surface area of the AC (1707 m<sup>2</sup> g<sup>-1</sup>) was found to be about twelve-fold the one of the commercial GO flakes (144 m<sup>2</sup> g<sup>-1</sup>). The low specific surface area obtained for GO flakes is consistent with other literature data [21, 24], and can be attributed to the stacking, folding, crumpling or pillaring of the layer (or multilayer) graphene plates during processing operations of graphene-based materials, which results in complex porous structures with surface areas considerably lower than the theoretical one (2600 m<sup>2</sup> g<sup>-1</sup>) [25]. Despite the low specific surface area of the solid GO used in this work, it is worth mentioning that, in our experimental work, the GO flakes were dispersed in water with the aid of sonication prior to its use in the D $\mu$ SPE procedure. The



sonication process provides a way to break the aggregates and to increase the proportion of single- or few-layers of graphene oxide in solution, therefore increasing the surface area of the adsorbent and modifying its porous structure with respect to the results reported in Table S1 for the commercial (not dispersed) GO flakes.

The morphology of the adsorbents can be appreciated in the SEM and TEM micrographs shown in Fig. S2. Fig. S2(a) and S2(b) correspond to the SEM and TEM micrographs, respectively, of the activated carbon, where its granular and amorphous morphology can be observed. The SEM and TEM micrographs of Fig. S2(c) and S2(d), respectively, correspond to graphene oxide. The SEM image of Fig. S2(c) shows the wrinkling and aggregation of the solid graphene oxide sheets, while the TEM micrograph of Fig. S2(d) shows the layered morphology of this sorbent when dispersed in water by sonication.

The surface functional groups of both AC and GO adsorbents, identified by FTIR analysis, are presented in Fig. S3. The graphene oxide FTIR-ATR spectrum in this Fig shows the characteristic bands of C-O-C at  $\sim 1030\text{ cm}^{-1}$ , C-O at  $\sim 1230\text{ cm}^{-1}$ , C=C at  $\sim 1620\text{ cm}^{-1}$  and C=O at  $\sim 1720\text{ cm}^{-1}$ . The band in the region of  $3600\text{--}3300\text{ cm}^{-1}$  is attributed to the O-H stretching vibrations of hydroxyl and carboxyl groups of GO [26]. By contrast, the activated carbon shows a comparatively flat FTIR-ATR spectrum.

### 3.2 Optimization of D $\mu$ SPE(AC) and D $\mu$ SPE(GO) procedures

Several experimental factors affecting metals extraction by D $\mu$ SPE (*i.e.* extraction time, pH and adsorbent amount) were optimized by using univariate optimization modality. In those D $\mu$ SPE procedures including a metal complexation step, the concentration of the complexing agent was always fixed at 0.5% (w/w), which is a concentration well in excess the stoichiometric one needed to chelate all metals in the test samples. In all the optimization studies, test samples consisted in model aqueous solutions containing  $1\text{ }\mu\text{g}\cdot\text{g}^{-1}$  of the different analytes.

#### 3.2.1 Optimization of the D $\mu$ SPE(AC) procedure

Fig. 3 shows the results obtained in the optimization of the D $\mu$ SPE(AC). The y-axis in the graphs corresponds to the normalized integrated intensity (in percentage) of the different analyte emission lines obtained from LIBS analysis of the analyte-enriched adsorbents, whereas error bars correspond to the percent relative standard deviation (% RSD) of three independent replicate measurements. For the sake of clarity, only error bars for the element showing the largest RSD are shown in the graphs. In any case, measurement precision ranged between about 2-9 % RSD in all the optimization studies.

Extraction time (Fig. 3(a)) was studied within the time interval of 1 to 20 minutes. In these experiments, the adsorbent amount was fixed at  $500\text{ }\mu\text{g}$  and the extraction pH was set at 6.5. As can be observed from Fig. 3(a), a minimum of 10 min extraction time was needed for the analytes lines to reach maximum emission signal. After 20 min extraction time, emission signals were observed to remain approximately constant within the limits of experimental error for three of the metals (Cd, Cr and Ni), whereas a slight decrease was observed for the other three (Mn, Zn and Pb). Consequently, 10 min extraction time was selected as optimum condition for the following experiments.

Solution pH plays an important role in the extraction of the chelated metals on activated carbon. On the one hand, sample acidity has a strong influence on the stability of the metal-DDTC chelates and, on the other hand, the medium pH affects the surface charge of the activated carbon and, therefore, the

adsorbate-adsorbent interactions during the adsorption process [27]. In this work, the effect of the pH on analyte extraction was examined in the range of pH from 5 to 9.5. It can be seen from Fig. 3(b) that the most intense emission signals were obtained in the pH interval of 6-7 for most of the analytes with exception of Ni and Cr, for which this interval extended to higher pH values (*i.e.*, from 6 to 8). In any case, emission signal was observed to peak at the same pH of 6 for all the metals and, therefore, this was the value selected as optimum.

Results obtained in the optimization of the adsorbent amount are shown in Figure 3(c). This optimization study was performed by varying the amount of activated carbon added to the sample from 100  $\mu\text{g}$  to 500  $\mu\text{g}$ . After extraction, the solids were prepared for LIBS analysis following the same procedure described in Section 2.3.2 above. However, in this case, the diameter of the silicon moulds used as containers for the analyte-enriched adsorbents was adjusted according to the adsorbent amount to be analysed in each experiment, with the intention to allow the solid to fill the entire base of the circular mould. Thus, the diameter of the silicon moulds was gradually increased from  $\sim 2$  mm to  $\sim 4$  mm when the adsorbent amount was increased from 100  $\mu\text{g}$  to 500  $\mu\text{g}$ . For comparative purposes, LIBS analysis of the different amounts of adsorbent was always carried out by averaging the same number of laser shots. This number was limited by the lowest quantity of adsorbent tested (*i.e.*, 100  $\mu\text{g}$ ), which allowed a maximum of 20 averaged laser shots (*i.e.*, 5 different surface locations with 4 shots in each location). It can be seen from Figure 3(c) that emission signals increased with the AC amount, showing a maximum at 400  $\mu\text{g}$  followed by a decrease at 500  $\mu\text{g}$ . A raise in extraction efficiency with adsorbent amount is typical in D $\mu$ SPE processes and can be attributed to the increment of the surface area available for adsorption. However, this initial improvement is usually observed to level-off after exceeding a given quantity of adsorbent [28-31], which disagree with the trend observed in Figure 3(c). A possible hypothesis for this anomalous behaviour could be a self absorption effect occurring during LIBS analysis of the analyte enriched solid. The adsorption capacity of activated carbon normally exceeds 1  $\text{mg g}^{-1}$  [32-34]. By assuming this minimum adsorption capacity, the concentration of analytes in the solid after extraction could reach, for the worst estimation, 0.1%. This concentration can be considered high enough to start producing self-absorption effects in a laser induced plasma [35].

Summarizing the above discussion, the selected optimum experimental conditions for D $\mu$ SPE(AC) were 10 minutes of extraction time, solution pH of 6 and 400  $\mu\text{g}$  of adsorbent.

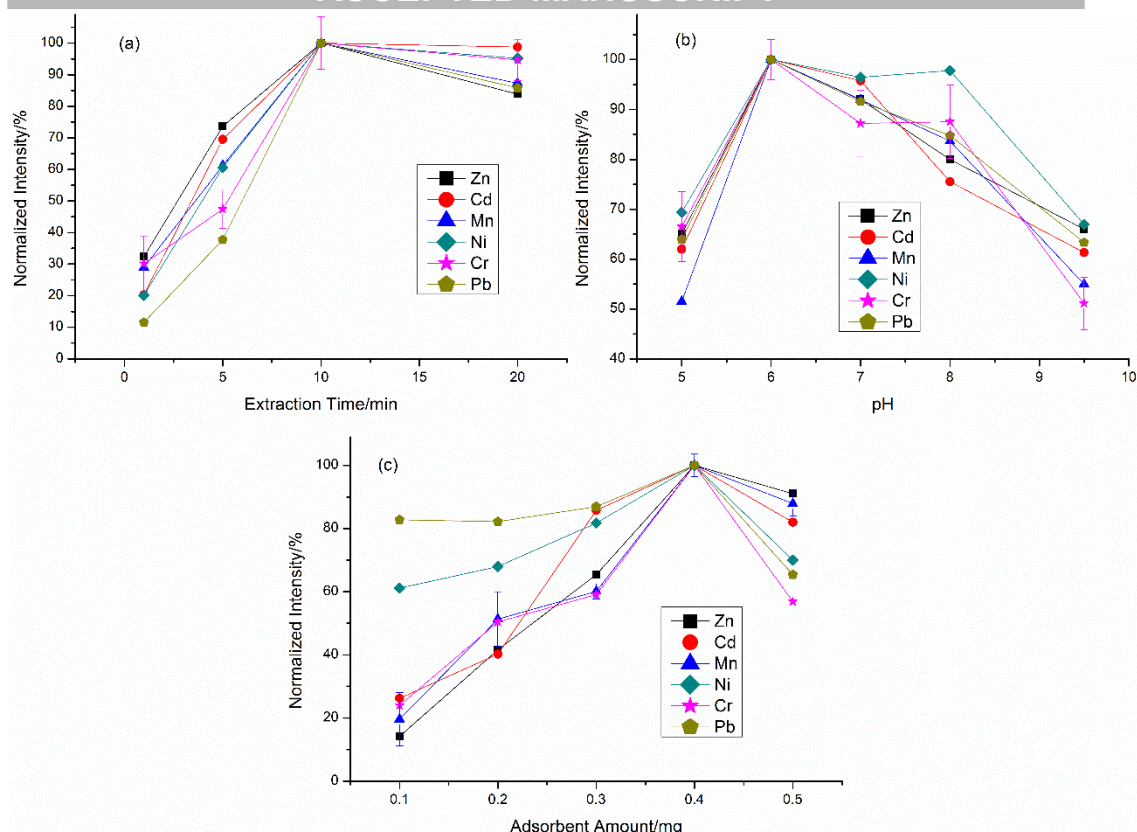


**Fig. 3** Results obtained in the optimization of the different parameters affecting the D $\mu$ SPE(AC) procedure: (a) Extraction time, (b) pH and (c) adsorbent amount. [DDTC]: 0.5%. Only error bars for the element showing the largest RSD values are shown.

### 3.2.2 Optimization of the D $\mu$ SPE(GO) procedure

Figure 4 shows the results obtained in the optimization of the D $\mu$ SPE(GO) procedure. Optimization of the extraction time is presented in Figure 4(a). In these experiments, adsorbent amount and solution pH were fixed at 400  $\mu$ g and 6, respectively. As observed, a shorter extraction time was needed for the analyte lines to reach maximum emission signal compared to that obtained with D $\mu$ SPE(AC) procedures (*i.e.*, 5 min (GO) *vs* 10 min (AC)). However, contrary to D $\mu$ SPE(AC) results, emission signals using D $\mu$ SPE(GO) were observed to drop sharply at extraction times longer than 5 min. Consequently, a precisely controlled extraction time of 5 min was selected as the optimum for all subsequent experiments.

After optimization of the extraction time, the next study was focused on the sample pH which, as in D $\mu$ SPE(AC) procedures, is a crucial experimental parameter in D $\mu$ SPE(GO). Solution pH affects the surface chemistry of the GO due to ionization equilibrium of the different oxygen-containing functional groups (*e.g.*, carboxyl or hydroxyl groups). Low pH values lead to a positively charged graphene oxide surface because of protonation of the functional groups, whereas high pH values induce negatively charged surface due to deprotonation. The pH at which the surface charge of the adsorbent is zero is denoted as point of zero charge ( $pH_{pzc}$ ). This implies that pH values above the  $pH_{pzc}$  of the GO will lead to a negatively charged surface, resulting in conditions that are more favourable for interaction with positively charged metal ions [36, 37]. Besides its influence on the adsorbent surface chemistry, pH also affects the proportion of the various metal ion species present in solution due to hydrolysis (*e.g.*,  $M^{2+}$ ,  $M(OH)^+$ ,  $M(OH)_2$ ,  $M(OH)_3^-$ , ...). At low pH values but still above the  $pH_{pzc}$  of the GO, the relative

proportion of  $M^{n+}$  is high, and metal ions adsorption can occur through several mechanisms, such as electrostatic attraction, ion exchange and/or surface complexation. At the other extreme (*i.e.*, highly alkaline conditions) the proportion of negatively charged metal species in solution increases (*e.g.*,  $M(OH)_3^-$  or  $M(OH)_4^{2-}$ ) and, due to electrostatic repulsion, these species are hardly adsorbed on the negatively charged binding sites of GO [21, 23, 37]. From the above discussion, it can be realised how pH conditions can affect, in an overall, the extraction of metal ions by GO. However, optimal solution pH for each metal may vary depending on several factors, such as the metal electronegativity or the stability constant of the metal hydroxide and/or metal carboxylate complex resulting from the interaction with functional groups of the GO surface.

In this work, adsorption of the metals was investigated in the pH interval between 4 and 9. The lowest pH condition was set at a value slightly above, or at least similar to, the  $pH_{pzc}$  usually characterizing GO adsorbents (*i.e.*,  $pH_{pzc}$  in the range 2.0 – 4.1) [20, 21, 36-38], in order to have positively charged surface conditions. Extractions were carried out with 400  $\mu g$  of adsorbent and 5 min extraction time. As observed from Figure 4(b), maximum adsorption was obtained at pH 5 for all the metals. Emission intensity of the different analytes was observed to decrease at increasing pH, although the signal decrease was more or less marked depending on the metal.

Figure 4(c) shows the results obtained in the optimization of the quantity of adsorbent. In these experiments, the analyte-enriched GO samples were prepared for LIBS analysis following the same procedure previously described in Section 3.2.1 for the optimization of the quantity of AC. However, in the case of GO, LIBS analysis of the different amounts of adsorbent was always carried out by averaging 12 laser shots (*i.e.*, 3 different surface locations with 4 shots in each location). As observed from Figure 4(c), the maximum emission signal for all the analytes was achieved with 300  $\mu g$  of GO, decreasing when increasing the amount of adsorbent. This behaviour is similar to that found in the optimization of the D $\mu$ SPE(AC) procedure, with the only difference of a slightly lower optimum value in the case of GO. As in D $\mu$ SPE(AC), self absorption could be a possible explanation of this phenomenon, which could be more marked for this adsorbent than for AC possibly due to a higher adsorption capacity of GO.

Summarizing the above results, the selected optimum experimental conditions for D $\mu$ SPE(GO) procedure were 5 minutes of extraction time, solution pH of 5 and 300  $\mu g$  of adsorbent.

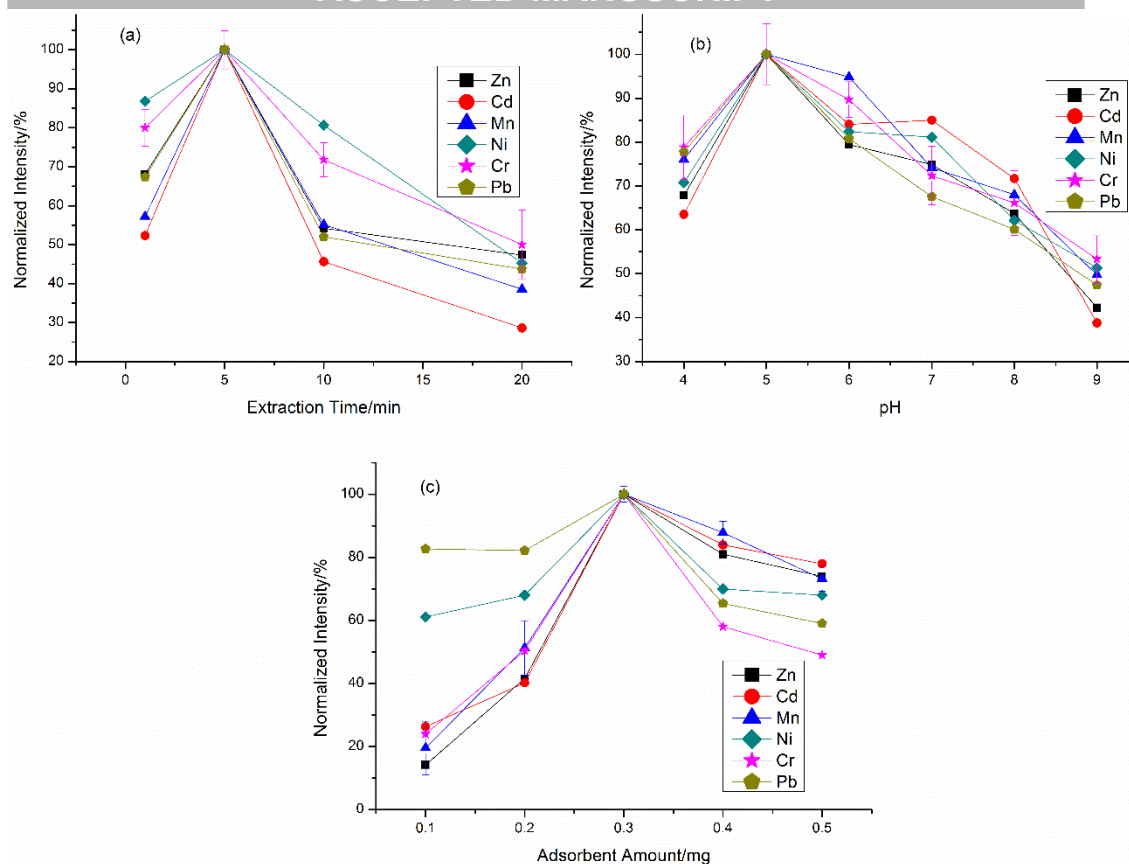


**Fig. 4** Results obtained in the optimization of the different parameters affecting the DμSPE(GO) procedure: (a) Extraction time, (b) pH and (c) adsorbent amount. Only error bars for the element showing the largest RSD values are shown

### 3.3 Analytical figures of merit of DμSPE(AC)-LIBS and DμSPE(GO)-LIBS procedures

Sensitivity, limit of detection (LOD), limit of quantification (LOQ) and signal repeatability were evaluated for both DμSPE(AC)-LIBS and DμSPE(GO)-LIBS procedures. To this end, five standard solutions with analyte concentrations in the range 0.05-1.00  $\mu\text{g g}^{-1}$  were analysed in order to obtain the corresponding calibration plots. DμSPE processes were always carried out under the selected optimum conditions for each adsorbent, whereas LIBS measurements of the analyte-enriched adsorbents were performed by averaging a number of pulses of 100 (*i.e.*, 10 surface locations with 10 shots per location) and 49 (*i.e.*, 7 surface locations with 7 shots per location) for AC and GO adsorbents, respectively. In all cases, calibration graphs were obtained from triplicate analysis of the standards. Sensitivity was evaluated from the slope of the calibration graphs. LOD and LOQ were calculated following the  $3\sigma$  and  $10\sigma$  IUPAC recommendation, respectively, with  $\sigma$  the standard deviation of six replicate analysis of the less concentrated standard (*i.e.*, 0.05  $\mu\text{g g}^{-1}$ ). The same replicate measurements of this standard were used to estimate the signal repeatability at the lowest concentration level, presented as percent relative standard deviation (% RSD). Table 1 summarizes the results obtained for both adsorbents, including additional information regarding linearity in the concentration interval evaluated (expressed as determination coefficient,  $R^2$ ), and relative values of sensitivity and LOD obtained with both procedures. As observed, calibration graphs presented good linearity independently of the adsorbent used in the microextraction step, with  $R^2$  values above 0.99 for all the analytes with exception of Ni (Table 1, Figure S4 and S5). Sensitivity was always higher with the use of DμSPE(GO)-LIBS, but this sensitivity improvement over

D $\mu$ SPE(AC)-LIBS was observed to be analyte-dependent (*i.e.*, about two-fold improvement for Cd, Mn and Ni, nearly six-fold for Zn and Pb, and about seventeenth-fold for Cr). A roughly similar trend was observed for the calculated LODs and LOQs. LODs obtained with D $\mu$ SPE(GO)-LIBS and D $\mu$ SPE(AC)-LIBS for Cd, Mn and Ni were practically identical, due to the insignificant differences in sensitivity and signal precision obtained with both procedures. However, D $\mu$ SPE(GO)-LIBS led to LOD improvements from 2 to 5-fold for the other three metals. Again, the highest LOD and LOQ improvement was obtained for Cr, with about a five-fold decrease. With both procedures and for all the analytes, the obtained LODs and LOQs were at the  $\mu\text{g kg}^{-1}$  level. LODs ranged from 25  $\mu\text{g}\cdot\text{kg}^{-1}$  (Cd) to 101  $\mu\text{g}\cdot\text{kg}^{-1}$  (Zn) with D $\mu$ SPE(AC)-LIBS, and from 8  $\mu\text{g}\cdot\text{kg}^{-1}$  (Cr) to 44  $\mu\text{g}\cdot\text{kg}^{-1}$  (Zn) when using D $\mu$ SPE(GO)-LIBS. Signal repeatability at 50  $\mu\text{g}\cdot\text{kg}^{-1}$  concentration level was below 8 % RSD in all cases, with D $\mu$ SPE(GO)-LIBS providing similar or better % RSD values compared to D $\mu$ SPE(AC)-LIBS.

A comparison of this method with previously published works involving SPE-LIBS procedures is shown in Table 2. As observed, the proposed D $\mu$ SPE procedure with the use of graphene oxide leads to lower limits of detection than those obtained in previously published works for almost all the analytes tested, with exception of Mn. In the case of Cr, a similar limit of the detection was obtained by Wang *et al.* [18]. However, compared to Wang *et al.* method, the proposed D $\mu$ SPE(GO) has the advantage of a greater simplicity, since metal complexation is not needed. The SPE method proposed by Youli *et al.* [43], consisting in the use of ordinary paper as adsorbent, also led to good limits of detection for Cr and Pb, but with the use of extraction times as long as three hours. Lee *et al.* [44], by using a SPE method similar to that of Youli *et al.* but with only 5 min extraction time, obtained much higher limits of detection. The same authors succeeded in reducing the limits of detection for Cr and Pb at the low  $\mu\text{g kg}^{-1}$  level, but with the use of a completely different sample preparation procedure in which 40 ml of sample, containing a submerged piece of paper, was heated to dryness in an oven at 150°C for one hour. Afterwards, the paper was analysed by LIBS. Even if this is an interesting procedure for reducing the limits of detection of LIBS for the analysis of liquids, it is also time consuming and, in addition, it could be hardly adapted for an automatic system of analysis.

In the light of the previously presented results and due to the advantages of D $\mu$ SPE(GO)-LIBS over D $\mu$ SPE(AC)-LIBS regarding experimental simplicity, experiments for trueness evaluation were only performed with the GO-based methodology. Trueness was evaluated from recovery experiments. To this end, a real sample of tap water collected from the municipal water system of the area of San Vicente del Raspeig in Alicante (Spain) was spiked with 0.2  $\mu\text{g}\cdot\text{g}^{-1}$  of the different analytes. Unspiked and spiked samples were analysed in triplicate by D $\mu$ SPE(GO)-LIBS in order to calculate the relative spike recovery according to the equation:

$$R = \frac{\bar{x}' - \bar{x}}{x_{\text{spike}}} \times 100 \quad (1)$$

With  $\bar{x}'$  the mean value of the concentration found in the spiked sample,  $\bar{x}$  the mean value of the concentration found in the unspiked sample and  $x_{\text{spike}}$  the added concentration.

It is worth mentioning that the water sample used for trueness evaluation can be classified as “very hard water” attending to its hardness value ( $\sim 34^\circ\text{F}$ , with a concentration of Ca and Mg of  $\sim 73 \text{ mg}\cdot\text{L}^{-1}$  and  $37 \text{ mg}\cdot\text{L}^{-1}$ , respectively) [48]. Nevertheless, as observed from Table 3, quite acceptable recoveries



were obtained for the different analytes, with recovery values ranging from 98 % for Ni to 110 % for Zn and Cr. In addition, a statistical *t*-test performed at 95 % confidence level revealed no significant differences between found and fortified concentrations. These results indicate that under the experimental conditions used in this work, D $\mu$ SPE(GO)-LIBS methodology was relatively free from matrix effects, given the high concentration level of possible interfering ions in the analysed sample.

#### 4. Conclusions

In this work, two D $\mu$ SPE procedures performed with the use of activated carbon and graphene oxide as adsorbent materials were evaluated as sample preparation methods for LIBS analysis of aqueous samples. The presented results demonstrate that the resulting measurement procedures (*i.e.*, D $\mu$ SPE(AC)-LIBS and D $\mu$ SPE(GO)-LIBS) are suitable for the detection of several analytes of environmental interest in water samples at the  $\mu\text{g kg}^{-1}$  concentration level. Even if sensitive elemental analysis can be successfully achieved with both measurement procedures, D $\mu$ SPE(GO)-LIBS provides, in general terms, superior analytical capabilities than D $\mu$ SPE(AC)-LIBS regarding sensitivity, LOD and LOQ. In addition, the use of graphene oxide as adsorbent material in the D $\mu$ SPE procedure can offer the added benefit of a greater experimental simplicity, due to the elimination of the metals complexation step from the microextraction process. With the use of D $\mu$ SPE(GO)-LIBS, the obtained LODs and LOQs were below  $50 \mu\text{g kg}^{-1}$  and  $150 \mu\text{g kg}^{-1}$ , respectively, for all the analytes under study, and the method trueness was demonstrated by analysis of a real sample of tap water characterized by a high hardness level, resulting in recovery values between 98 % and 110 %. Even so, and in order to definitively assess the analytical performance of the D $\mu$ SPE(GO)-LIBS method, a detailed investigation of the effect of possible coexisting ions in water samples should be carried out in further studies.

As a general conclusion, it can be said that the use of GO as adsorbent can provide a substantial advance towards the simplification of SPME procedures as sample preparation methods for LIBS analysis of liquids. However, the developed D $\mu$ SPE(GO)-LIBS methodology is still far from being easily implementable in an automatic analytical system. On the one hand, the two independent processes of D $\mu$ SPE and LIBS detection are difficult to combine in an automatic way. On the other hand, the D $\mu$ SPE procedure is by itself difficult to automate. These difficulties can be solved with the use of an alternative SPME configuration, such as TFME, which is easily automatable and can be simply combined with LIBS detection. This possibility is currently under study in our laboratory.

#### Acknowledgements

This work was supported by the Spanish Ministry of Economy and Competitiveness [project number CTQ2016-79991-R and fellowship number BES-2012-058759 (FPI-MICINN)]; the Regional Government of Valencia (Spain) [project number PROMETEO/2013/038]; and the University of Alicante [grant number UAUSTI16-04]. The authors want to express their gratefulness to Prof. Ángel Linares for the provision of the activated carbon canister.

## References

- [1] F. Pena-Pereira, Miniaturization in sample preparation, in: F. Pena-Pereira (Eds.), From conventional to miniaturized analytical systems, De Gruyter Open, 2014, pp 1-28.
- [2] D.A. Cremers, J.L. Radziemski, Handbook of laser induced breakdown spectroscopy, John Wiley & Sons, Ltd., West Sussex, 2006.
- [3] V. Lazic, Laser-induced breakdown spectroscopy, in: S. Musazzi, U. Perini (Eds.), LIBS analysis of liquids and of materials inside liquids, Springer Series in Optical Sciences 182, Springer-Verlag, Berlin Heidelberg, 2014, pp 195-225.
- [4] A. Ruas, A. Matsumoto, H. Ohba, K. Akaoka, I. Wakaida, Application of laser-induced breakdown spectroscopy to zirconium in aqueous solution, Spectrochim. Acta B. 131 (2017) 99–106.
- [5] A. Kuwako, Y. Uchida, K. Maeda, Supersensitive detection of sodium in water with use of dual-pulse laser-induced breakdown spectroscopy, Appl. Opt. 42 (2003) 6052-6056.
- [6] K. Rifai, S. Laville, F. Vidal, M. Sabsabi, M. Chaker, Quantitative analysis of metallic traces in water-based liquids by UV-IR double-pulse laser-induced breakdown spectroscopy, J. Anal. At. Spectrom. 27 (2012) 276-283.
- [7] S. Groh, P.K. Diwakar, C.C. Garcia, A. Murtazin, D.W. Hahn, K. Niemax K, 100% efficient sub-nanoliter sample introduction in laser-induced breakdown spectroscopy and inductively coupled plasma spectrometry: implications for ultralow sample volumes, Anal. Chem. 82 (2010) 2568-2573.
- [8] S. Zhong, R. Zheng, Y. Lu, K. Cheng and J. Xiu, Ultrasonic nebulizer assisted LIBS: a promising metal elements detection method for aqueous sample analysis, Plasma Sci. Tech. 17 (2015) 979-984.
- [9] V.N. Rai, F.Y. Yueh, J.P. Singh, Time-dependent single and double pulse laser-induced breakdown spectroscopy of chromium in liquid, Appl. Opt. 47 (2008) G21-G29.
- [10] M. Sadegh, S.H. Tavassoli, Quantitative analysis of toxic metals lead and cadmium in water jet by laser-induced breakdown spectroscopy, Appl. Opt. 50 (2011) 1227-1233.
- [11] S. Zhong, Y. Lu, W-J. Kong, K. Cheng, R. Zheng, Quantitative analysis of lead in aqueous solutions by ultrasonic nebulizer assisted laser induced breakdown spectroscopy, Front. Phys. 11 (2016) 114202.
- [12] Z. Chen, H. Li, M. Liu, R. Li, Fast and sensitive trace metal analysis in aqueous solutions by laser-induced breakdown spectroscopy using wood slice substrates, Spectrochim. Acta B 63 (2008) 64–68.
- [13] X. Wang, Y. Wei, Q. Lin, J. Zhang, Y. Duan, Simple, fast matrix conversion and membrane separation method for ultrasensitive metal detection in aqueous samples by laser-induced breakdown spectroscopy, Anal. Chem. 87 (2015) 5577–5583.
- [14] H. Bagheri, H. Piri-Moghadam, M. Naderi, A. Es'haghi, A. Roostaie, Miniaturization in sample preparation, in: F. Pena-Pereira (Eds.) Solid-Phase Microextraction and Related Techniques, De Gruyter Open, 2014, pp 29-87.



- [15] B. Socas-Rodríguez, A.V. Herrera-Herrera, M. Asensio-Ramos, J. Hernández-Borges, *Analytical Separation Science*. Volume 5, in: J. L. Anderson, A. Berthod, J. Pino-Estévez, A. M. Stalcup (Eds.) *Dispersive Solid-Phase Extraction*, Wiley-VCH, Weinheim, Germany, 2015, pp 1525–1570.
- [16] T. Khezeli, A. Daneshfar, Development of dispersive micro-solid phase extraction based on micro and nano sorbents, *Trends Anal. Chem.* 89 (2017) 99–118.
- [17] L. Xu, Q. Qi, X. Li, Y. Bai, H. Liu, Recent advances in applications of nanomaterials for sample preparation, *Talanta* 146 (2016) 714–726.
- [18] X. Wang, L. Shi, Q. Lin, X. Zhu, Y. Duan, Simultaneous and sensitive analysis of Ag(I), Mn(II), and Cr(III) in aqueous solution by LIBS combined with dispersive solid phase micro-extraction using nano-graphite as an adsorbent, *J. Anal. At. Spectrom.* 29 (2014) 1098–1104.
- [19] X. Wang, B. Liu, Q. Lu, Q. Qu, Graphene-based materials: Fabrication and application for adsorption in analytical chemistry, *J. Chromatogr. A* 1362 (2014) 1–15.
- [20] Y. Bian, Z-Y. Bian, J-X. Zhang, A-Z. Ding, S-L. Liu, H. Wang, Effect of the oxygen-containing functional group of graphene oxide on the aqueous cadmium ions removal, *Appl. Surf. Sci.* 329 (2015) 269–275.
- [21] G. Zhao, X. Ren, X. Gao, X. Tan, J. Li, C. Chen, Y. Huang, X. Wang, Removal of Pb(II) ions from aqueous solutions on few-layered graphene oxide Nanosheets, *Dalton Trans.* 40 (2011) 10945–10952.
- [22] H. Wang, X. Yuan, Y. Wu, H. Huang, G. Zeng, Y. Liu, X. Wang, N. Lin, Y. Qi, Adsorption characteristics and behaviors of graphene oxide for Zn(II) removal from aqueous solution, *Appl. Surf. Sci.* 279 (2013) 432–440.
- [23] R. Sitko, E. Turek, B. Zawisza, E. Malicka, E. Talik, J. Heimann, A. Gagor, B. Feist, R. Wrzalik, Adsorption of divalent metal ions from aqueous solutions using graphene oxide, *Dalton Trans.* 42 (2013) 5682–5689.
- [24] P. Li, H. Gaoc, Y. Wang, Uptake of Ni(II) from aqueous solution onto graphene oxide: Investigated by batch and modelling techniques, *J. Mol. Liq.* 227 (2017) 303–308.
- [25] F. Guo, M. Creighton, Y. Chen, R. Hurt, I. Külaots, Porous structures in stacked, crumpled and pillared graphene-based 3D materials, *Carbon* 66 (2014) 476–484.
- [26] J. Chen, B. Yao, C. Li, G. Chi, An improved Hummers method for eco-friendly synthesis of graphene oxide, *Carbon* 64 (2013) 225–229.
- [27] T. Karanfil, Activated Carbon Surfaces in Environmental Remediation, in: T. J. Bandosz (Eds.) *Activated carbon adsorption in drinking water treatment*, first ed., Elsevier Ltd., Amsterdam, The Netherlands, 2016, pp 345–375.
- [28] B. Feist, Selective dispersive micro solid-phase extraction using oxidized multiwalled carbon nanotubes modified with 1,10-phenanthroline for preconcentration of lead ions, *Food Chem.* 209 (2016) 37–42.

- [29] H. Shirkhanloo, A. Khaligh, H.Z. Mousavi, A. Rashidi, Ultrasound assisted-dispersive-micro-solid phase extraction based on bulky amino bimodal mesoporous silica nanoparticles for speciation of trace manganese (II)/(VII) ions in water samples, *Microchem. J.* 124 (2016) 637–645.
- [30] M. Krawczyk, M. Jeszka-Skowron, Multiwalled carbon nanotubes as solid sorbent in dispersive microsolid-phase extraction for the sequential determination of cadmium and lead in water samples, *Microchem. J.* 126 (2016) 296–301.
- [31] M. Ghazaghi, H. Shirkhanloo, H.Z. Mousavi, A.M. Rashidi, Ultrasound-assisted dispersive solid phase extraction of cadmium(II) and lead(II) using a hybrid nanoadsorbent composed of graphene and the zeolite clinoptilolite, *Microchim. Acta* 182 (2015) 1263–1272.
- [32] H. Sadegh, G.A.M. Ali, V.K. Gupta, A.S.H. Makhlof, R. Shahryari-ghoshekandi, M.N. Nadagouda, M. Sillanpa, E. Megiel, “The role of nanomaterials as effective adsorbents and their applications in wastewater treatment”, *J. Nanostruct. Chem.* 7 (2017) 1-14.
- [33] Renu, M. Agarwal, K. Singh, “Heavy metal removal from wastewater using various adsorbents: a review”, *J. Water Reuse Desal.* 7 (2017) 387-419.
- [34] M.M. Rahman, M. Adil, A.M. Yusof, Y.B. Kamaruzzaman, R.H. Ansary, “Removal of heavy metal ions with acid activated carbons derived from oil palm and coconut shells, *materials* 7 (2014) 3634-3650.
- [35] I.B. Gornushkin, J.M. Anzano, L.A. King, B.W. Smith, N. Omenetto, J.D. Winefordner, “Curve of growth methodology applied to laser-induced plasma emission spectroscopy”, *Spectrochim. Acta B* 54 (1999) 491-503.
- [36] G. Zhao, J. Li, X. Ren, C. Chen, X. Wang, Few-layered graphene oxide nanosheets as superior sorbents for heavy metal ion pollution management, *Environ. Sci. Technol.* 45 (2011) 10454–10462.
- [37] W. Peng, H. Li, Y. Liu, S. Songm, A review on heavy metal ions adsorption from water by graphene oxide and its composites, *J. Mol. Liq.* 230 (2017) 496–504.
- [38] J. Huang, Z. Wu, L. Chen, Y. Sun, Surface complexation modelling of adsorption of Cd(II) on graphene oxides, *J. Mol. Liq.* 209 (2015) 753–758.
- [39] N.E. Schmidt, S.R. Goode, “Analysis of aqueous solutions by laser-induced breakdown spectroscopy of ion exchange membranes”, *Appl. Spectrosc.* 56 (2002) 370-374.
- [40] Z. Chen, H. Li, M. Liu, R. Li, “Fast and sensitive trace metal analysis in aqueous solutions by laser-induced breakdown spectroscopy using wood slice substrates”, *Spectrochim. Acta B* 63 (2008) 64-68.
- [41] S. Sawaf, W. Tawfik, “Analysis of heavy elements in water with high sensitivity using laser induced breakdown spectroscopy”, *Optoelectron. Adv. Mater. Rapid Commun.* 8 (2014), 414-417.
- [42] G. Niu, Q. Shi, M. Xu, H. Lai, Q. Lin, K. Liu, Y. Duanc, “Dehydrated carbon coupled with laser-induced breakdown spectrometry (LIBS) for the determination of heavy metals in solutions”, *Appl. Spectrosc.* 69 (2015) 1190-1198.

- [43] Y. Youli, Z. Weidong, Q. Huiguo, S. Xuejiao, R. Ke, “Simultaneous determination of trace lead and chromium in water using laser-induced breakdown spectroscopy and paper substrate”, *Plasma Sci. Technol.* 16 (2014) 683-687.
- [44] Y. Lee, S-W. Oh, S-H. Han, “Laser-induced breakdown spectroscopy (LIBS) of heavy metal ions at the sub-parts per million Level in water”, *Appl. Spectrosc.* 66 (2012) 1385-1396.
- [45] W. Guanhong, S. Duixiong, S. Maogen, D. Chenzhong, “LIBS detection of heavy metal elements in liquid solutions by using wood pellet as sample matrix”, *Plasma Sci. Technol.* 16 (2014) 598- 601.
- [46] D. Zhu, J. Chen, J. Lu, X. Ni, “Laser-induced breakdown spectroscopy for determination of trace metals in aqueous solution using bamboo charcoal as a solid-phase extraction adsorbent”, *Anal. Methods* 4 (2012) 819-823.
- [47] Z. Chen, Y. Godwal, Y.Y. Tsui, R. Fedosejevs, “Sensitive detection of metals in water using laser-induced breakdown spectroscopy on wood sample substrates”, *Appl. Opt.* 49 (2010) C87-C94.
- [48] (35) Aguas municipales de Alicante, Analysis of water quality in the municipal water system of San Vicente del Raspeig (Alicante, Spain). <http://www.aguasdealicante.es/AnalisisAgua/>, 2018 (accessed 18 April 2018).

**Table 1.** Analytical figures of merit obtained with the D $\mu$ SPE(AC)–LIBS and D $\mu$ SPE(GO)–LIBS procedures

Parameters	Zn		Cd		Mn		Ni		Cr		Pb	
	AC	GO	AC	GO	AC	GO	AC	GO	AC	GO	AC	GO
R <sup>2</sup> <sup>a</sup>	0.99	0.99	0.99	0.99	0.99	0.99	0.98	0.98	0.99	0.99	0.99	0.99
	19	16	07	10	28	26	63	81	36	19	26	32
Sensitivity/ct	82	441	106	243	824	182	261	552	116	199	243	158
s·g· $\mu$ g <sup>-1</sup> ab	$\pm 4$	$\pm$	$\pm 5$	$\pm$	$\pm$	3 $\pm$	$\pm$	$\pm$	$\pm 5$	2 $\pm$	$\pm$	6 $\pm$
		20		12	35	77	15	32		90	10	61
LOD/ $\mu$ g·kg <sup>-1</sup>	101	44	25	24	34	36	43	40	41	8	57	21
LOQ/ $\mu$ g·kg <sup>-1</sup>	337	147	85	79	112	119	145	133	136	28	190	71
Repeatability /%RSD <sup>c</sup>	7.9	3.5	6.1	5.7	7.4	7.8	5.8	5.4	7.1	1.5	7.3	2.7
Relative sensitivity <sup>d</sup>		5.4		2.3		2.2		2.1		17.2		6.5
Relative LOD <sup>e</sup>		2.3		1.1		0.9		1.1		4.9		2.7

<sup>a</sup> Number of calibration points, N=5

<sup>b</sup> Value  $\pm$  standard deviation

<sup>c</sup> Relative standard deviation, n=6, analyte concentration 0.05  $\mu$ g·g<sup>-1</sup>

<sup>d</sup> Sensitivity GO / Sensitivity AC

<sup>e</sup> LOD<sub>AC</sub>/LOD<sub>GO</sub>

**Table 2:** Comparison with LODs reported in previously published references involving SPE-LIBS

Element	Wavelength (nm)	Extraction procedure Procedure (adsorbent) – Experimental details	LOD ( $\mu$ g L <sup>-1</sup> )	Reference
Zn	472.2	SPE (ion exchange membrane) - filtration of 10 mL	850	[39]
	202.5	D $\mu$ SPE (activated carbon) - 5 min stirring	101	This work
	202.5	D $\mu$ SPE (graphene oxide) - 5 min stirring	44	This work
Cd	361.1	SPE (ion exchange membrane) - filtration of 10 mL	210	[39]
	508.6	SPE (Wood slices) - 2 min immersion	59	[40]

	214.4	D $\mu$ SPE (activated carbon) - 5 min stirring	25	This work
	214.4	D $\mu$ SPE (graphene oxide) - 5 min stirring	24	This work
Mn	403.1	D $\mu$ SPE (nano-graphite) - 2 min stirring	10.85	[18]
	255.1	SPE (Wood slices) - 2 min immersion	36	[40]
	403.3	SPE (Wood slices) - 5 min immersion	623	[41]
	259.4	D $\mu$ SPE (activated carbon) - 5 min stirring	34	This work
	259.4	D $\mu$ SPE (graphene oxide) - 5 min stirring	36	This work
Ni	353.0	SPE (ion exchange membrane) - filtration of 10 mL	310	[39]
	352.5	D $\mu$ SPE (activated carbon) - 5 min stirring	43	This work
	352.5	D $\mu$ SPE (graphene oxide) - 5 min stirring	40	This work
Cr	425.4	D $\mu$ SPE (nano-graphite) - 2 min stirring	9.51	[18]
	427.5	DSPE (Dehidrated carbón) -30 min stirring	460	[42]
	427.5	SPE (ordinary paper) - 180 min immersion	26	[43]
	267.7	SPE (ordinary paper) - 5 min immersion	360	[44]
	267.7	Evaporation of 40 mL sample in an oven – 60 min	18	[44] <sup>a</sup>
	425.4	SPE (Wood pellets) – 120 min immersion	130	[45]
	425.4	SPE (Wood slices) - 2 min immersion	34	[40]
	520.9	SPE (ion exchange membrane) - filtration of 10 mL	130	[39]
	357.9	D $\mu$ SPE (activated carbon) - 5 min stirring	41	This work
	357.9	D $\mu$ SPE (graphene oxide) - 5 min stirring	8	This work
Pb	405.8	DSPE (Dehidrated carbón) -30 min stirring	65	[42]
	405.8	DSPE (Bamboo charcoal) - 30 min stirring	8500	[46]
	405.8	SPE (ordinary paper) - 180 min immersion	33	[43]
	220.3	SPE (ordinary paper) - 5 min immersion	2700	[44]
	220.3	Evaporation of 40 mL sample in an oven – 60 min	75	[44] <sup>a</sup>
	405.8	SPE (wooden stirrer sticks) - 15 min immersion	113	[47]
	405.8	SPE (Wood slices) - 2 min immersion	74	[40]
	405.8	SPE (ion exchange membrane) - filtration of 10 mL	1100	[39]
	368.3	D $\mu$ SPE (activated carbon) - 5 min stirring	57	This work
	368.3	D $\mu$ SPE (graphene oxide) - 5 min stirring	21	This work

<sup>a</sup> ordinary paper was submerged in 40 mL of solution and the solution was heated to dryness in an oven at 150°C for one hour. SPE was not performed.

**Table 3.** Recovery values obtained in the analysis of a real sample of tap water with the use of the D $\mu$ SPE(GO)–LIBS analytical methodology

Analyte	Added conc./ $\mu\text{g}\cdot\text{g}^{-1}$	Found conc./ $\mu\text{g}\cdot\text{g}^{-1}$	Recovery/%
Zn	0.000	– <sup>a</sup>	
	0.200	$0.221 \pm 0.012$	110
Cd	0.000	– <sup>a</sup>	
	0.200	$0.197 \pm 0.009$	99
Mn	0.000	– <sup>a</sup>	
	0.200	$0.210 \pm 0.015$	105
Ni	0.000	– <sup>a</sup>	
	0.200	$0.196 \pm 0.021$	98
Cr	0.000	– <sup>a</sup>	
	0.200	$0.219 \pm 0.007$	110
Pb	0.000	– <sup>a</sup>	
	0.200	$0.218 \pm 0.010$	109

<sup>a</sup> Not detected

## Highlights

- D $\mu$ SPE-LIBS, using graphene oxide as sorbent, has been evaluated for the first time
- Several metals in liquid samples has been detected at  $\mu\text{g Kg}^{-1}$  level by LIBS
- Metal chelation step has been avoided with the use of graphene oxide
- Graphene oxide provides superior analytical capabilities than activated carbon